Biosensors and Bioelectronics 136 (2019) 23–30

Contents lists available at ScienceDirect

Biosensors and Bioelectronics

journal homepage: www.elsevier.com/locate/bios

Vancomycin functionalized WO_3 thin film-based impedance sensor for efficient capture and highly selective detection of Gram-positive bacteria

Sanjay Singh[a], Akshay Moudgil[b], Nishant Mishra[a,b], Samaresh Das[b], Prashant Mishra[a,*]

[a] Department of Biochemical Engineering and Biotechnology, Indian Institute of Technology Delhi, Hauz Khas, New Delhi, 110016, India
[b] Centre for Applied Research in Electronics, Indian Institute of Technology Delhi, Hauz Khas, New Delhi, 110016, India

ARTICLE INFO

Keywords:
Vancomycin
Gram-positive bacteria
Impedance sensor
WO_3 thin film

ABSTRACT

In this study, we report a facile, reusable, and highly sensitive label-free impedance sensor for discriminating Gram-positive and Gram-negative bacteria. The impedance sensor was fabricated using gold interdigitated electrodes onto a tungsten oxide thin film. X-Ray diffraction confirmed the formation of polycrystalline tungsten oxide. Field emission scanning electron microscopy and atomic force microscopy revealed that tungsten oxide has a porous structure. Tungsten oxide was functionalized with vancomycin, a glycopeptide antibiotic known to have a specific interaction with the peptidoglycan layer of Gram-positive bacteria. Fourier transform infrared microscopy and scanning electron microscopy were employed to test the morphological coating of vancomycin on interdigitated electrodes/tungsten oxide sensor. The functionalized tungsten oxide sensor was highly efficient in the capture of Gram-positive bacteria. The impedance measurement was also sensitive to differentiate between viable and non-viable Gram-positive bacteria. Limit of detection 10^2 colony forming unit/ml, linear dynamic range 10^2–10^7 colony forming unit/ml under physiological conditions and reusable nature of this vancomycin coated impedance sensor provide a label-free strategy for quick, sensitive and highly selective detection of Gram-positive bacteria.

1. Introduction

Rapid, sensitive and selective detection of bacteria holds great promise in control of disease propagation as it can help decide the course of treatment. It can also help to monitor the antibiotic resistance, the spread of hospital acquired infections and contamination of surgical instruments. The traditional protocol of bacterial detection involves the culture and colony counting, and various biochemical tests but is time consuming and requires larger sample volumes. This has led to the development of various newer, more sensitive methods based on nucleic acid amplification (Brakstad et al., 1992), immuno-assays (Freed et al., 1982), surface plasmon resonance (Koubová et al., 2001), surface enhanced Raman spectroscopy (Kumar et al., 2015; Lu et al., 2013) as well as various electrochemical methods (Wang et al., 2011).

Amongst the available techniques, electrochemical impedance spectroscopy is quite promising due to its simplicity, scalability, low cost and high sensitivity (10–10^9 colony forming unit/ml (CFU/ml)). A number of electrochemical sensors – both label and label-free have been developed in the past for the detection of pathogens such as *E. coli* (Xu et al., 2016). Antibodies immobilized on gold nanoparticles (Barreiros dos Santos et al., 2013; Wang et al., 2013) and ITO (Barreiros dos Santos et al., 2015; Ruan et al., 2002; Yang et al., 2004a,b) have shown improved sensitivity and specificity. The other biological materials used for functionalization of electrodes were lectin (Yang et al., 2016) and antimicrobial peptide (Li et al., 2014; Hoyos-Nogués et al., 2016; Etayash et al., 2014). Recently biological materials such as proteins (Kalyani et al., 2017; Moudgil et al., 2018b) have also been used to develop electronics.

However, most impedance-based sensors employ bacteria-specific antibodies for the specific detection of only a single species of pathogen (Barreiros dos Santos et al., 2013; Barreiros dos Santos et al., 2015; Yang et al., 2004a,b; Wang et al., 2013) and these antibodies are relatively of very large size. These antibody-based methods have limitations as they have several functional groups and their binding to the surface depends on their orientation on the surface (Soukka et al., 2001). Antibodies also have limited storage stability (Templier et al., 2016; Etayash et al., 2014). Thus, smaller molecular probes such as vancomycin (van) (Lin et al., 2005), mannose (Lin et al., 2002) and antimicrobial peptides (Etayash et al., 2014; Hoyos-Nogués et al., 2016) have attracted considerable interest to capture bacteria specifically. Nonetheless, rapid and affordable techniques to differentiate between Gram-positive and Gram-negative bacteria are needed to help reduce

* Corresponding author.
E-mail address: pmishra@dbeb.iitd.ac.in (P. Mishra).

https://doi.org/10.1016/j.bios.2019.04.029
Received 26 February 2019; Received in revised form 5 April 2019; Accepted 15 April 2019
Available online 19 April 2019
0956-5663/

antimicrobial resistance and to reduce the prescription of large doses of broad-spectrum antibiotics.

In this regard, vancomycin, a glycopeptide antibiotic known to be efficient against mainly Gram-positive bacteria has shown huge potential (Kell et al., 2008; Liu et al., 2011). Interestingly, various studies demonstrate the interaction of vancomycin with D-alanyl-D-alanine terminus of peptidoglycan extending from the cell wall of Gram-positive bacteria (Kell et al., 2008; Wang et al., 2018). This antibiotic does not penetrate the outer membrane of Gram-negative bacteria and hence remains ineffective against them. This preferential binding of vancomycin has been exploited for capture and differentiation of bacteria using vancomycin functionalized silver nanorod array-based SERS (Liu et al., 2011; Wu et al., 2015). Additionally, vancomycin has been shown to be stable at room temperature for 26 days in solution (Ensom et al., 2010).

In addition to different materials for impedance sensors, various strategies have been employed to functionalize them. Earlier, ITO functionalized with antibodies (Barreiros dos Santos et al., 2015; Ruan et al., 2002; Yang et al., 2004a,b), gold electrode functionalized with lectin (Yang et al., 2016), streptavidin (Xu et al., 2016) and antimicrobial peptides (Li et al., 2014) have been developed to improve the specific detection of bacteria using impedance-based sensors.

Recently, Zn-CuO nanoparticle and graphene oxide nanosheet deposited Ni porous electrode based impedance sensor has been developed for bacterial capture with high sensitivity (Wu et al., 2018). Nevertheless, metal oxide nanostructures are of great relevance for biosensing due to porous morphology, better conformation, desired orientation and high binding functionality. Metal oxide materials exhibit high charge transfer rate and enhanced adsorption property (Topoglidis et al., 1998), providing the desired environment for immobilization of biomolecules and resulting increased sensitivity for biodetection (Solanki et al., 2011).

Amongst metal oxide materials, tungsten oxide (WO_3) is a wide band gap material having various applications in photocatalysis (Kwon et al., 2000), photoelectrochemistry (Ohno et al., 1998), photodetection (Moudgil et al., 2018a), batteries (Li and Fu, 2010) and gas sensing (Zeng et al., 2012). The properties of WO_3 have been shown to depend on its morphology: mainly size, shape, porosity and structure (Deb, 1973). The nanoporous structure of WO_3 has shown enhanced sensitivity for the analyte detection (Barsan et al., 2016; Siciliano et al., 2008; Hu et al., 2012) and similar enhanced sensitivity has been reported for other transition metal oxides (Topoglidis et al., 1998).

WO_3 is a new and effective material for fabrication of impedance devices due to its tunable electrical behaviour with a band gap of 2.6 eV–3.3 eV. In addition, the presence of oxygen vacancies provides electrical conductivity (Bringans et al., 1981; Owen et al., 1978). So far this material has not been employed for developing impedance-based biosensors. In the present work, vancomycin functionalized WO_3 thin film-based sensor has been exploited for efficient capture and selective detection of Gram-positive bacteria using *S. aureus* as a model organism.

2. Methods

2.1. Device fabrication

The interdigitated gold electrodes (IDE) were fabricated on the tungsten oxide/silicon-dioxide/silicon ($WO_3/SiO_2/Si$). The thickness of thermally grown SiO_2 on the Si wafer was 1 μm. Then a 20 nm thin film of tungsten (W) was deposited using radio-frequency (RF) sputtering at 15 mTorr. The polycrystalline tungsten trioxide (WO_3) was obtained after placing the sample in the furnace at 800 °C for 4 h in the presence of O_2/N_2. This was followed by a standard lithography process to pattern the WO_3/Au-IDE structures (WO_3 IDE sensor). The Au electrodes having 5 μm width, 30 μm pitch and 1800 μm length were obtained by Cr/Au deposition (15nm/80 nm).

2.2. Functionalization of WO_3 with vancomycin

WO_3 IDE sensor was immersed in a piranha solution (containing H_2SO_4 and 30% H_2O_2 (3: 1 v/v)) for 2 min. After thoroughly rinsing with ultrapure water (18.2 MΩ) (Purelab Option-Q, Elga, UK) and ethanol (Merck, USA), this sensor was dried with gaseous nitrogen. The freshly cleaned WO_3 IDE sensor was immersed in absolute ethanol and ultrasonicated for 5 min and dried with gaseous nitrogen. The WO_3 IDE sensor was then incubated with half the minimum inhibitory concentration (MIC) of vancomycin for respective bacteria for 1 h at room temperature to functionalize the WO_3 IDE sensor uniformly. This functionalized sensor was rinsed several times with ultrapure water and phosphate buffer saline (PBS) (pH 7.4, 10 mM) to remove unbound vancomycin.

2.3. Bacterial strains and culture conditions

Escherichia coli ATCC 25922, *Staphylococcus aureus* ATCC 9144, *Pseudomonas aeruginosa* ATCC 14886, *Bacillus subtilis* ATCC 6633, *Pseudomonas ovalis NRRL B-85, Pseudomonas fluorescens NCIM, Bacillus licheniformis NRRL 1001 and Bacillus polymyxa DSM 366* were grown at 37 °C overnight at 150 rpm in Luria Broth (LB) from HI media, India. Next 10^6 cells were subcultured for 2–3 h to get the cells in the exponential phase. These cells were pelleted by centrifugation at $1073 \times g$ for 10 min and then re-suspended in 1 ml of PBS to obtain 10^8 CFU/ml as described in earlier works (Goel and Mishra, 2018; Jaiswal and Mishra, 2018). For further experiments, the cells were diluted with PBS or 0.9% NaCl or Foetal Bovine Serum (FBS) to the desired concentration of cells (10^2–10^8 CFU/ml) to test the effect of media and physiological conditions on impedance, respectively.

2.4. Cell viability assay

To study the effect of viability of Gram-positive bacteria on impedance, firstly these cells were treated using ultrasonication (Vibracell, SONICS, US) for 15 min at 5 s ON/5 s OFF pulse mode with frequency of 20 KHz (Joyce et al., 2003; Allison et al., 1996; Herceg et al., 2013) and were pelleted at $6708 \times g$ for 10 min. The cells were washed with PBS to remove media and finally re-suspended in PBS for viability assay using impedance measurements. The results were confirmed using plating and colony counting method as described by Clinical and Laboratory Standards Institute, USA (CLSI, 2015).

2.5. Characterization of vancomycin functionalized electrode

The WO_3 thin film was characterized using UV-Vis spectroscopy (PerkinElmer, Singapore) and X-Ray diffraction (XRD) (Rigaku Ultima IV, USA) to confirm the formation of polycrystalline thin film WO_3. Field emission scanning electron microscopy (FESEM) (JEOL, USA) was used to analyse the surface morphology of WO_3 thin film. Fourier Transform Infrared microscopy (FTIR) (Nicolet iN10, Thermofisher Scientific, US) was used to analyse the chemical groups present on the surface of WO_3 IDE sensor before and after vancomycin functionalization. The vancomycin functionalized region on the sensor was selected using an optical microscope connected to FTIR, and measurements were made in the mid-IR region from 400 to 4000 cm^{-1}. Energy dispersive X-ray spectroscopy (EDX) (Hitachi Tabeltop Microscope Model TM 3000, Japan) was employed for the elemental analysis of the sensor before and after functionalization with vancomycin. *S. aureus* at 10^2 CFU/ml were visualized in vancomycin coated WO_3 IDE sensor by scanning electron microscope (SEM) (Zeiss EVO 50, Carl Zeiss, Germany). The samples were fixed using 2% glutaraldehyde solution, then air-dried, gold-coated, and viewed under SEM at different magnifications. The roughness of the WO_3 IDE sensor surface before and after coating with vancomycin was analyzed using Atomic Force Microscopy (AFM) (Innova, Bruker, Singapore) in an area of 1 μm × 1 μm.

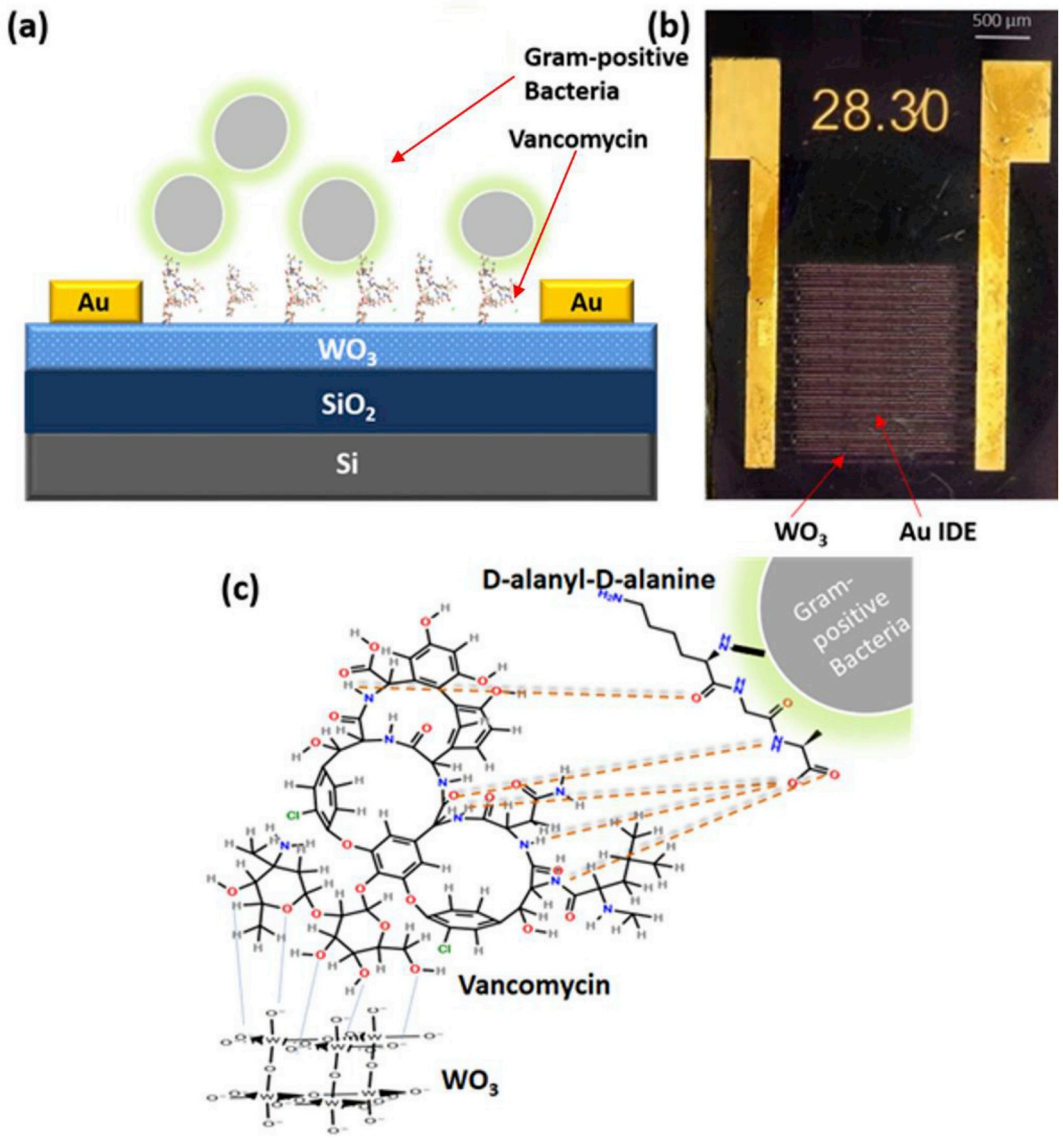

Fig. 1. (a) Schematic representation of vancomycin functionalized WO_3 IDE sensor showing Gram-positive bacteria binding with vancomycin functionalized on WO_3 IDE (cross-sectional view). (b) Optical image of the device with 5 µm width, 30 µm pitch, 1800 µm length and 28.30 represents the device number. (c) Illustration of the interaction of the backbone of vancomycin - D-alanyl-D-alanine of bacterial surface and binding of vancomycin to WO_3 surface.

2.6. Bacterial impedance measurements

The vancomycin functionalized WO_3 IDE sensor was treated with 4 µl of PBS, FBS and 0.9% NaCl solution containing different concentrations of bacterial samples. The WO_3 IDE sensor was then rinsed with PBS to remove unbound bacteria. The electrochemical impedance was measured in a solution containing 5 mM $K_4Fe(CN)_6$ and $K_3Fe(CN)_6$ using an alternating sinusoidal potential with an amplitude of 10 mV. Impedance spectra were recorded in the frequency range from 0.1 Hz to 1 MHz using a Biologic SP150 scientific analyzer at room temperature. All measurements were repeated at least three times to obtain consistent results.

3. Results and discussion

3.1. Fabrication and characterization of vancomycin functionalized electrodes

As illustrated in Fig. 1(a) vancomycin was used to functionalize the WO_3 IDE sensor surface upon which Gram-positive bacteria bind. Adsorption and non-covalent interactions play a significant role in immobilization of vancomycin on WO_3 thin film surface. WO_3 has a net positive charge due to oxygen vacancies (Bai and Zhou, 2014; Gillet et al., 2003) whereas vancomycin has a small negative charge at neutral pH (Pfeiffer, 1981) thus coulomb forces are responsible for the functionalization (Chen et al., 2012). Biological probes such as antibodies have been previously shown to be immobilized by adsorption on metal oxide without the use of a linker molecule (Li et al., 2008; Solanki et al., 2011; Topoglidis et al., 1998).

An optical image of the sensor is shown in Fig. 1(b) which represents the WO_3 IDE sensor with device number on the wafer. The device has a dimension of 5 µm width, 30 µm pitch and 1800 µm length fabricated on the Si/SiO_2 substrate. Fig. 1(c) shows the schematic of binding of the heptapeptide backbone of vancomycin with D-alanyl-D-alanine of the Gram-positive bacterial surface by hydrogen bonds with a high binding affinity (Rao et al., 1997; Sundram et al., 1996). Thus vancomycin is well suited for efficient capture and high specificity towards the Gram-positive bacteria (Hubbard and Walsh, 2003).

The WO_3 thin film was characterized by X-ray diffraction (XRD) and UV absorbance spectra. The distinct peaks of XRD pattern shown in Fig. 2(a),

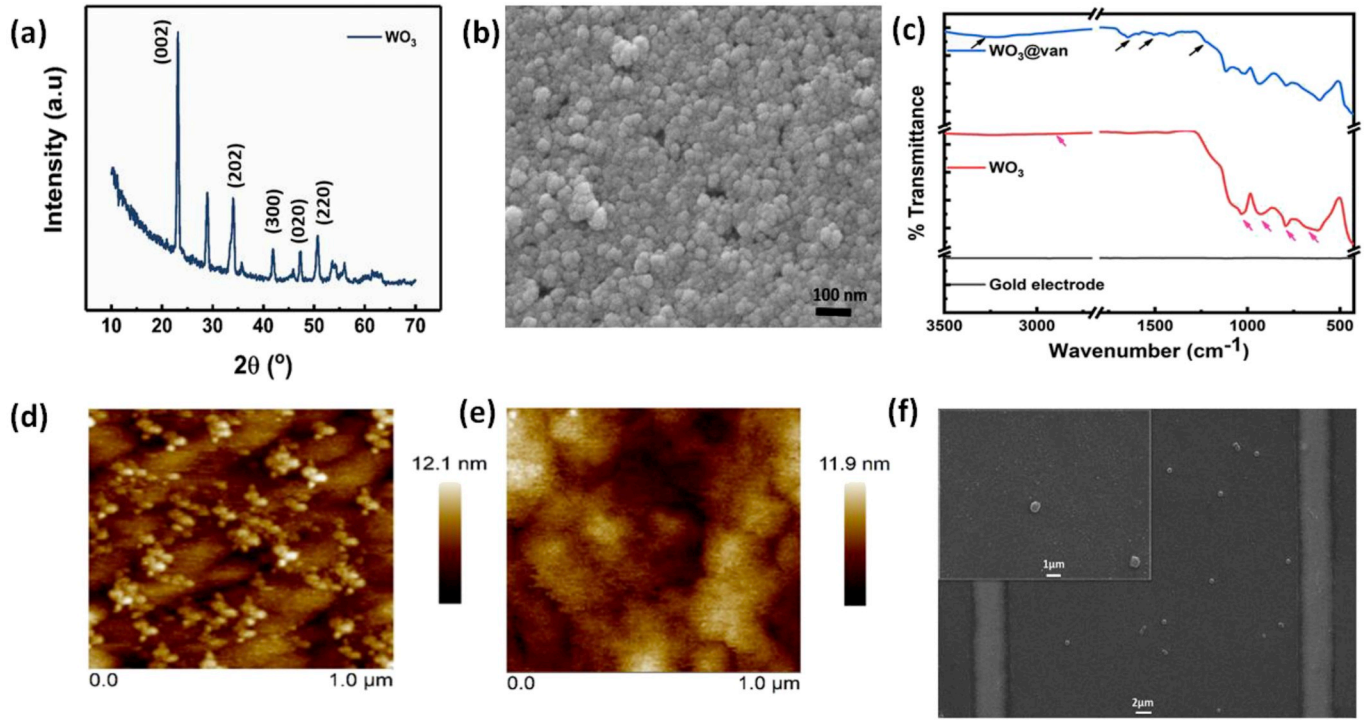

Fig. 2. (a) X-ray diffraction (XRD) pattern of WO_3. (b) FESEM image of WO_3. (c) FTIR spectra of Vancomycin functionalization WO_3, Pristine WO_3 and gold electrode. AFM image of (d) pristine WO_3 showing porous nanostructure and (e) vancomycin coated WO_3 IDE sensor. (f) SEM image (7000 X) of *S. aureus* at 10^2 CFU/ml on vancomycin coated WO_3 IDE sensor and inset showing *S. aureus* at higher magnification (25000 X). (For interpretation of the references to colour in this figure legend, the reader is referred to the Web version of this article.)

confirm the polycrystalline WO_3 thin film formation (Moudgil et al., 2018a). The band gap of WO_3 is 2.8 eV as depicted from UV absorbance spectra in Fig. S1 (supplementary content). The morphology of WO_3 with porous structure is shown in Fig. 2(b) using field emission scanning electron microscopy (FESEM). The FTIR spectra of different segments of the vancomycin functionalized WO_3 IDE sensor (Fig. 2(c)), and their corresponding images from where spectra were obtained are shown in Fig. S2 (i) (supplementary content). FTIR spectra for WO_3, peaks at 730 cm^{-1} and 910 cm^{-1} are attributed to stretch vibration (O-W^{6+}-O) as reported earlier (Zhang et al., 2011). The sharp band around 1030 cm^{-1} is due to asymmetric stretching vibrations (W=O) bonds (Zhang et al., 2013). A small peak at 2932 cm^{-1} corresponds to –OH group of WO_3. For vancomycin coated WO_3, peaks at 3450 cm^{-1}, 1680 cm^{-1}, 1505 cm^{-1} and 1230 cm^{-1} represent -OH, C=O, C=C and aromatic phenol in vancomycin, respectively (Yang et al., 2011). FTIR peaks for WO_3 as well as vancomycin functionalized WO_3 are well characterized and corroborate with earlier works (Zhang et al., 2011, 2013; Yang et al., 2011). This can be clearly seen in the (Fig. S2 (ii) (supplementary content)), magnified version of FTIR plot. No significant peaks were observed for the gold electrode. Thus the FTIR spectra suggest that there is successful functionalization of vancomycin on WO_3 IDE sensor.

The AFM image shows pristine WO_3 Fig. 2(d) and vancomycin functionalized WO_3 IDE sensor Fig. 2(e). The images were taken on a surface area of 1 μm × 1 μm. These images provided information on the shape and size of the grains of WO_3 thin film as well as their distribution in the aggregates. AFM images of WO_3 exhibit a porous morphology comprising of grains with sizes in the range of 40–70 nm which was also confirmed by FESEM as shown in Fig. 2(b). Vancomycin was directly used to functionalize the WO_3 surface. Fig. 2(e) exhibits that the roughness of the WO_3 IDE sensor decreases after functionalization with vancomycin. Our experiments have demonstrated that after removing non-specifically bound vancomycin by washing, the vancomycin attached to WO_3 surface remains bound even after several steps of subsequent washing. The functionalized sensors were used after removal of excess of vancomycin. This fact is demonstrated by the energy dispersive X-ray spectroscopy (EDX) data shown in Fig. S3 (supplementary content), where even after the first step of washing, the peaks of nitrogen (N_2) which is an elemental constituent of vancomycin, remain constant. This confirms the fact that vancomycin remains attached to the surface of WO_3 even after washing several times which is apparent from the reusability of the device.

Fig. 2(f) shows SEM images of the Gram-positive bacteria, *S. aureus* on vancomycin functionalized WO_3 IDE sensor. At 7000 X magnification, *S. aureus* was seen between the electrodes. Inset of Fig. 2(f), shows *S. aureus* clearly visible at a higher magnification (25000 X).

3.2. Bacterial impedance measurements

In impedance sensing, a frequency dependent excitation signal (U (ω)) was applied to the device and response was measured in the current I (ω). Initial calibration was done using open and short circuit operation of the instrument. Then the complex impedance Z (ω) is calculated using equation (1), where ω is the frequency and $j = \sqrt{-1}$.

$$Z(\omega) = \frac{U(\omega)}{I(\omega)} = Z_{re} + jZ_{im} \quad (1)$$

Measurements were performed over a frequency range of 0.1 Hz–1MHz, using an alternating sinusoidal potential with an amplitude of 10 mV and direct current bias of 0 V applied to the contact electrodes. The Bode plot (Fig. 3(a)), Nyquist plot (Fig. 3(b)) and phase change (Fig. 3(c)) of impedance spectra were plotted for *S. aureus*.

Initially, impedance spectrum in pristine condition was recorded, which acts as the reference of the WO_3 IDE sensor. Then, upon the immobilization of vancomycin and application of PBS without any bacteria, the impedance gets reduced from 1600 Ω to 1058 Ω. The free ions present in the PBS led to an increase in conductance and a decrease in the impedance. After repeating the measurements under the same conditions, we observed similar values (± 1%) of impedance.

Now WO_3 IDE sensor was tested at different concentrations of *S. aureus*. A significant change in impedance with the increment in the

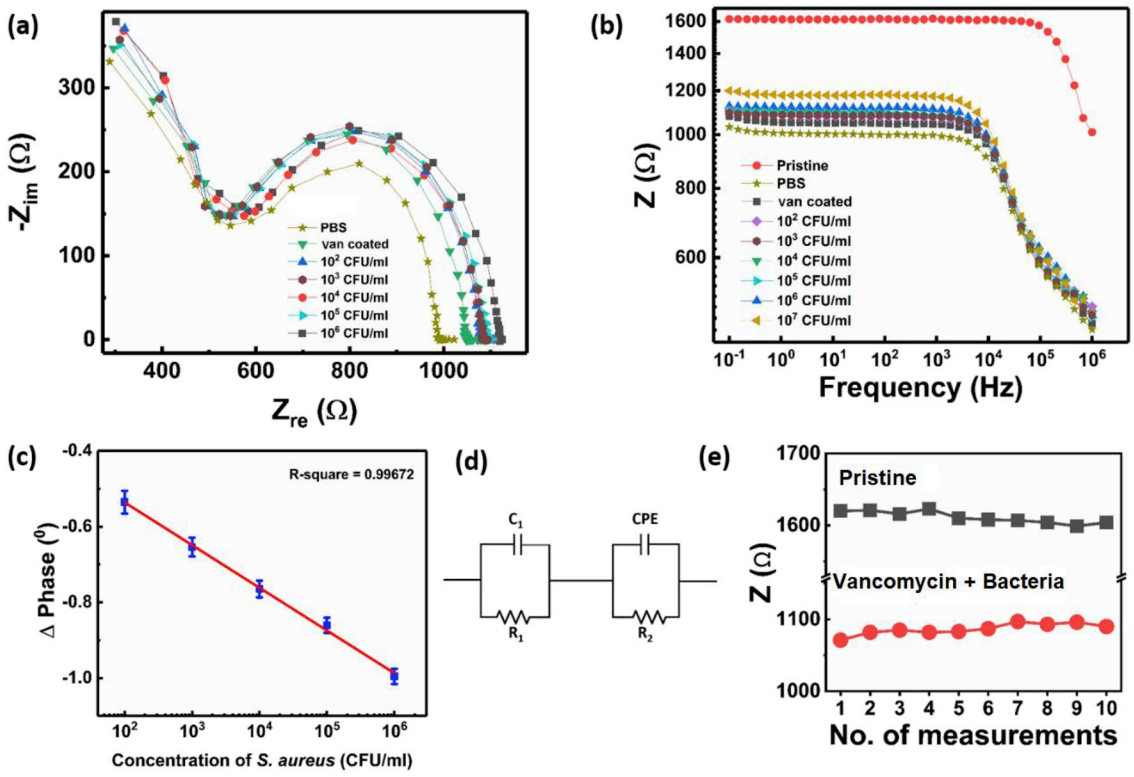

Fig. 3. Impedance measurement for different concentrations of *S. aureus* in PBS (pH 7.4, 10 mM) (a) Bode plot (b) Nyquist plot, (c) phase change (Data represent mean ± SD of 10 independent experiments) (d) Equivalent circuit model of the sensor and (e) repeatability of the device for ten measurements.

concentration of *S. aureus*, ranging from 10^2-10^7 CFU/ml was observed.

In the bode plot (Fig. 3(a)), the segment at low frequency corresponds to the diffusion process of the transport of redox species in the electrolyte to electrodes, and the segment at high frequency (up to 1 MHz) gives information about Faradaic electron transfer at the electrodes. The relative change in the phase with the increment in the concentration of *S. aureus* versus the control is shown in Fig. 3(c). The increment in phase change with *S. aureus* corresponds to the higher imaginary impedance (Z_{im}).

The equivalent electric circuit model shown in Fig. 3(d) was obtained to explain the physical origin of the measured output of the WO_3 IDE sensor. The output characterization results were fitted by applying the Powell algorithm in EIS spectrum analyzer tool. The extracted parameters of the equivalent electric circuit for *S. aureus* detection are shown in Table S1 (supplementary content) where R is a resistor, C is a capacitor, CPE is the constant phase element, n is CPE exponent and P is CPE pre-factor. R_1 represents the bulk resistance of the electrolyte solution whereas R_2 represents the charge transfer resistance.

The charge transfer resistance R_2 is very sensitive to the *S. aureus* and vancomycin interaction. As the concentration of *S. aureus* increased, the value of R_2 also increased which reflects the retardation of interfacial electron transfer kinetics (Ruan et al., 2002). This trend corresponds to the significant impedance of the charge transfer by the higher concentration of *S. aureus*. The defects and inhomogeneity in the WO_3 are represented by the CPE (Daniels and Pourmand, 2007), with exponent 'n' approaching 1 as depicted in Table S1 (supplementary content).

To test the repeatability of the WO_3 IDE biosensor, the impedance values were measured on pristine and vancomycin functionalized WO_3 IDE with Gram-positive bacteria for 10 different cycles of the experiment. Very minute differences were observed for the impedance value, as shown in Fig. 3(e). This suggests that the device is robust and can be used several times to detect pathogens.

3.2.1. *Efficient capture and selective detection of Gram-positive bacteria*

To find the limit of detection (LOD) of the WO_3 IDE sensor, the change in the impedance with respect to control (van) at different concentrations of *S. aureus* was extracted. The result of the ΔZ ($Z^{(van+bacteria)}$ - $Z^{(van)}$) as a function of *S. aureus* concentration is shown in Fig. 4(a). In the range of 10^2–10^6 CFU/ml, a linear relationship ΔZ = 8.515 (log [*S. aureus*]) + 13.914; R = 0.9857 was found. The LOD was calculated using equation; LOD = y + 3σ, where y is the charge transfer resistance value of PBS without bacteria and σ is the standard deviation (Miller and Miller, 2005).

The LOD of the WO_3 IDE sensor was calculated using change in impedance vs concentration plot of *S. aureus* (Fig. 4(a)) and found to be 29.49 Ω, which corresponds to *S. aureus* concentration < 10^2 CFU/ml. Hence, this biosensor is well suited for accurate detection of less than 100 CFU/ml of *S. aureus*. The low value of LOD is due to high affinity and selectivity of vancomycin functionalized WO_3 IDE for Gram-positive bacteria. Compared to previous works, the sensor in this study had either a smaller LOD or a wider linear dynamic range (Table S2 (supplementary content)).

Finally, the specificity of vancomycin functionalized IDE for the detection of *S. aureus* was tested by comparing the measured change of R_2 (van + bacteria) and R_2 (van) with respect to R_2 (van) value of all four Gram-positive and Gram-negative strains at 10^2 CFU/ml as shown in Fig. 4(b). All Gram-negative bacteria; *E. coli*, *P. aeruginosa*, *P. fluorescens and P. ovalis* act as non-targeted organisms, and hence the non-significant changes in spectra were obtained. Indeed, the specificity of the vancomycin coated IDE is mainly due to specific binding of vancomycin functionalized WO_3 IDE sensor to Gram-positive bacteria.

Measured percentage (%) change of R_2 (van + bacteria) and R_2 (van) with respect to control R_2 (van) of all four Gram-positive strains was found to be nearly 45–50%, whereas this change for Gram-negative strains was 3.5–4% (Fig. 4(b)) indicating high specificity of Gram-positive bacteria to bind to vancomycin coated WO_3 IDE sensor. The small value for Gram-negative bacteria may be due to non-specific binding.

Earlier methods used for the detection of bacteria were based on capture of specific bacteria to aptamer bound to different nanomaterials (Jia et al., 2014; Reich et al., 2017; Ranjbar and Shahrokhian, 2018;

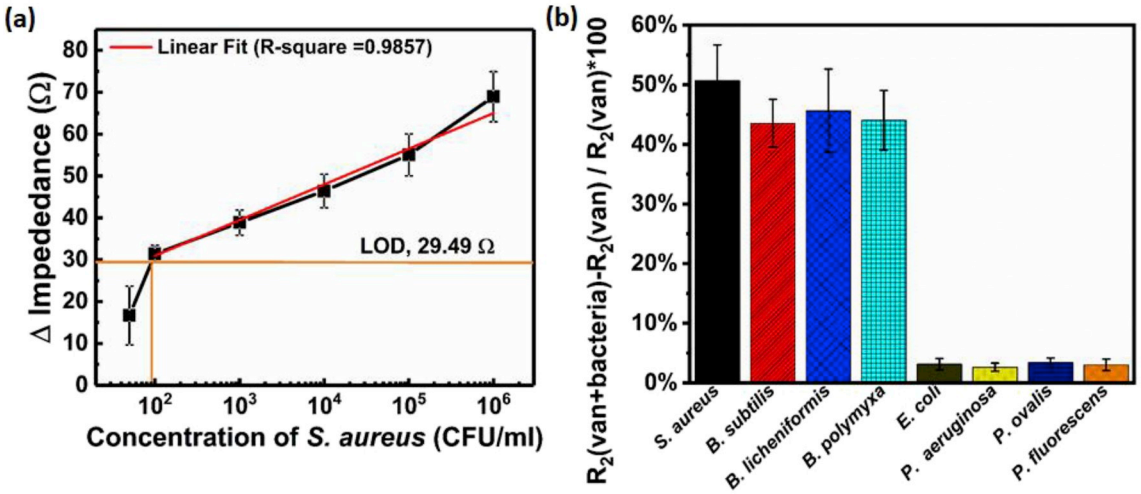

Fig. 4. (a) Impedance change at different concentrations of *S. aureus* with a limit of detection fitting. (b) Percentage (%) change between R_2 (van + bacteria) and R_2 (van) with respect to R_2 (van) for Gram-positive strains and Gram-negative strains at 10^2 CFU/ml bacterial concentration. R_2 represents the charge transfer resistance after vancomycin functionalization (van) and binding of bacteria (van + bacteria) which is very sensitive to the Gram-positive bacteria (*S. aureus*, *B. subtilis, B. polymyxa and B. licheniformis*) and vancomycin interaction. Data represent mean ± SD of 10 independent experiments.

Shahrokhian and Ranjbar, 2018), specific antibody (Barreiros dos Santos et al., 2015; Ruan et al., 2002; Yang et al., 2004a,b), lectin (Yang et al., 2016) and Magainin (Li et al., 2014) with variable specificity ranging from 1-10^3 CFU/ml. However, none of these methods was specific to a major class of bacteria. The device presented in this study can be used to discriminate between Gram-positive and Gram-negative bacteria for which the susceptibility to antibiotics is different. This sensor can thus help determine the course for antibiotic treatment.

Application of metal oxide thin film, WO_3 for developing impedance sensor (IDE) and its functionalization with vancomycin show lower limit of detection with higher selectivity towards Gram-positive bacteria. In addition, it has provided a rapid detection method (within 15 min) for discrimination of Gram-positive and Gram-negative bacteria.

3.3. Impedance measurement under physiological condition

In order to extend the usefulness of impedance measurements to physiological and clinical conditions, impedance was measured in FBS. Similar changes in the impedance were found when measurement performed in FBS as compared to in PBS, as shown in Nyquist plot and phase change plot of impedance (Fig. 5 (a) and 5(b)). The value of impedance increases with increase in the concentration of bacteria. This suggests that the fabricated antibiotic functionalized sensor could be used for accurate determination of *S. aureus* and other Gram-positive bacteria in samples with complex matrices like human serum. Cell concentration dependent changes in impedance have been observed earlier (Ward et al., 2018) in Luria Broth and in FBS suggesting the usefulness of impedance under physiological conditions.

To test the effect of growth medium, cells were spiked with 0.9% NaCl and impedance spectra before, and after incubation, in 0.9% NaCl for 3 h was recorded. Resistance peaks were observed at 1121 Ω and 1128 Ω as shown in Fig. 5(c). No significant change in the impedance before and after incubation with 0.9% NaCl was observed. This suggests that no growth takes place in *S. aureus* during first 3 h of incubation and supports the hypothesis that impedance change was related to cell density and growth. Similarly, earlier work has also demonstrated that incubation of bacteria in 0.9% NaCl has resulted in no change in impedance, unless 0.9% NaCl was spiked with different concentrations of bacteria (Ward et al., 2018). In some of the previous studies (Bonetto et al., 2014; Settu et al., 2015) impedance has been attributed to biofilm formation. In the present work, cells were grown for only 3 h. During this period biofilm formation does not occur. Thus impedance changes are attributed to the varying concentration of bacteria in the medium.

3.4. Cell viability assay of Gram-positive using impedance measurement

Rapid determination of live (viable) and dead (non-viable) bacteria is critical to maintain the efficacy of an antibiotic and to determine contamination in food samples. Recently a rapid method based on synchronous fluorescence has been developed for viability testing of bacteria (Li et al., 2018), nonetheless, a simple and facile method of viability test is required. High-power ultrasound at frequencies around 20 kHz can be used to kill bacteria. This has been a standard microbiology technique for many years to disrupt both Gram-positive and Gram-negative bacterial cells (Piyasena et al., 2003; Allison et al., 1996; Herceg et al., 2013). So, to investigate the ability of vancomycin coated WO_3 IDE sensor to discriminate between live and dead bacteria, 10^5 CFU/ml of *S. aureus* were ultrasonicated at 20 kHz (Joyce et al., 2003). Plating and colony counting method, which is a standard procedure given by Clinical and Laboratory Standards Institute, USA, (CLSI, 2015) was used to confirm the killing of bacteria (Viability test) before and after sonication. A 4 $\log_{10}$ reduction after sonication, confirms that bacteria were dead.

With ultrasonication, the cell wall of bacteria is damaged and the specific D-alanyl-D-alanine in the surface of the bacterial membrane is disintegrated due to which vancomycin binding to bacteria is disrupted. Moreover, lysis of cells leads to release of ionic metabolites which increase the conductance of the solution. Therefore compared to the non-sonicated (live) cells, the R_2 value gets decreased in sonicated (dead) cells as shown in Fig. 5(d).

4. Conclusions

In this study, we have fabricated a facile, sensitive and label-free impedance-based sensor employing vancomycin functionalized WO_3 IDE for the detection of Gram-positive bacteria, e.g. *S. aureus*. XRD confirmed the formation of crystalline WO_3 and FESEM revealed its porous morphology. FTIR and AFM revealed the morphological features of vancomycin coated WO_3 IDE sensor structure. The device has shown promising characteristics with a low limit of detection (80–100 CFU/ml) at 29.49 Ω and a wide linear range of detection 10^2–10^7 CFU/ml. The distinct feature of this sensor was the ability to differentiate between Gram-positive and Gram-negative bacteria due to the efficient capture of Gram-positive bacteria by vancomycin coated surface of WO_3 IDE sensor.

In addition, its ability to differentiate between live and dead Gram-positive bacteria was required for determination of contamination in food samples and hospital environments. Interestingly WO_3 IDE worked under

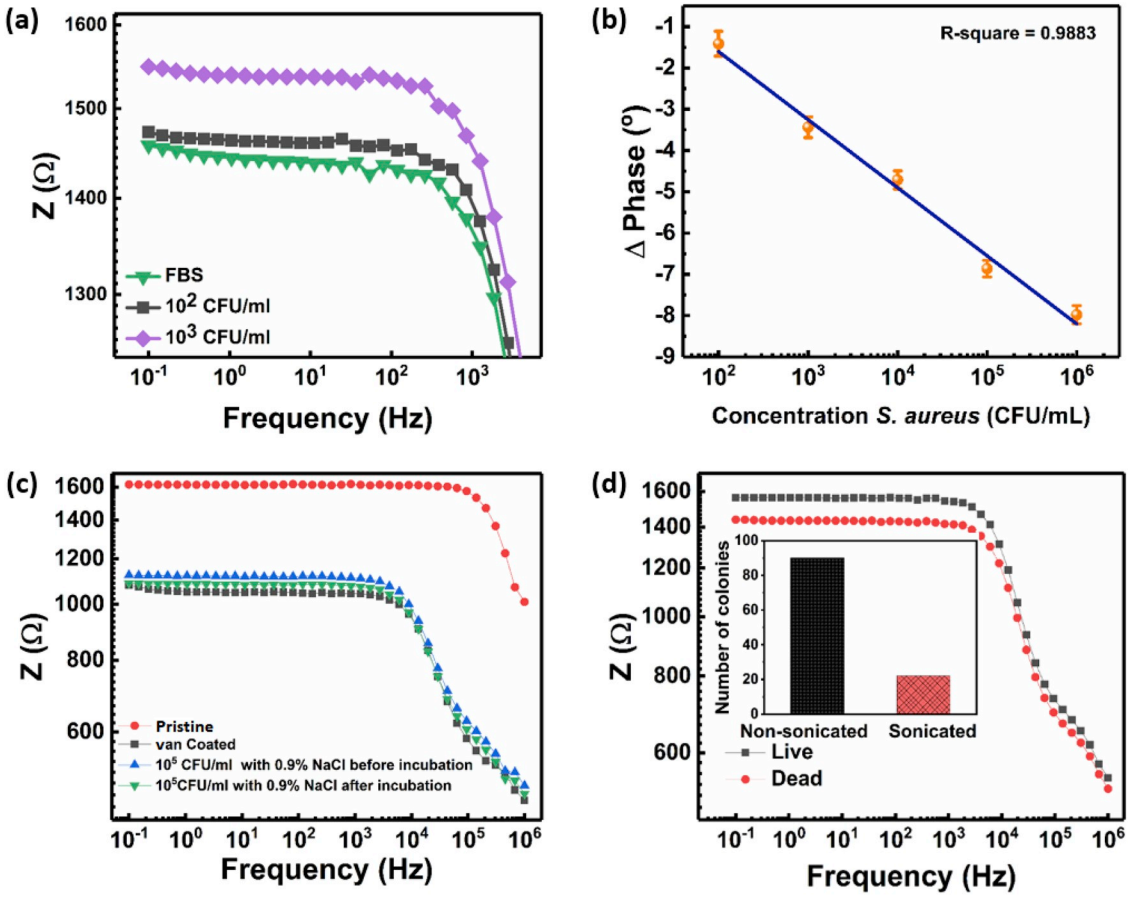

Fig. 5. Impedance measurement for different concentrations of *S. aureus* in FBS (a) Nyquist plot (b) phase change (Data represented as mean ± SD of 10 independent experiments). Impedance measurement in 0.9% NaCl before and after incubation of *S. aureus* (c) Nyquist plot. Impedance measurement of Dead/Live *S. aureus* (d) Nyquist plot of bacteria before and after sonication; inset represents colony forming units before (cells diluted from 10^5 to 10^2) and after sonication (undiluted) by plating and colony counting method.

physiological conditions such as in the presence of PBS and FBS. This sensor has great promise to be used with the minimum processing of clinical samples. Nonetheless, the complexity of various clinical samples and their effect on impedance needs to be further explored. Scalability and reusability of these sensors make them useful for practical applications.

CRediT authorship contribution statement

Sanjay Singh: Conceptualization, Methodology, Formal analysis, Investigation, Data curation, Visualization, Writing - original draft. **Akshay Moudgil:** Conceptualization, Methodology, Formal analysis, Investigation, Data curation, Visualization, Writing - original draft. **Nishant Mishra:** Conceptualization, Methodology, Formal analysis, Investigation, Data curation, Visualization, Writing - original draft. **Samaresh Das:** Conceptualization, Supervision, Project administration, Funding acquisition, Writing - review & editing. **Prashant Mishra:** Conceptualization, Supervision, Project administration, Funding acquisition, Writing - review & editing.

Acknowledgements:

Sanjay Singh and Akshay Moudgil acknowledge financial assistance from the Ministry of Human Resource and Development (MHRD) and Ministry of Electronics and Information Technology (MeitY), respectively. The project was partially funded by MeitY (5(1)/2017-NANO) and DST (DST/NM/NNetRA/2018(G)-IIT-D) grants of Government of India.

Appendix A. Supplementary data

Supplementary data related to this article can be found at https://doi.org/10.1016/j.bios.2019.04.029.

References

Allison, D.G., D'Emanuele, A., Eginton, P., Williams, A.R., 1996. The effect of ultrasound on *Escherichia coli* viability. J. Basic Microbiol. 36, 1–11.
Bai, J., Zhou, B., 2014. Titanium dioxide nanomaterials for sensor applications. Chem. Rev. 114, 10131–10176.
Barreiros dos Santos, M., Agusil, J.P., Prieto-Simón, B., Sporer, C., Teixeira, V., Samitier, J., 2013. Highly sensitive detection of pathogen *Escherichia coli* O157:H7 by electrochemical impedance spectroscopy. Biosens. Bioelectron. 45, 174–180.
Barreiros dos Santos, M., Azevedo, S., Agusil, J.P., Prieto-Simón, B., Sporer, C., Torrents, E., Juárez, A., Teixeira, V., Samitier, J., 2015. Label-free ITO-based immunosensor for the detection of very low concentrations of pathogenic bacteria. Bioelectrochemistry 101, 146–152.
Barsan, N., Staerz, A., Weimar, U., 2016. Understanding the potential of WO_3 based sensors for breath analysis. Sensors 16, 1815.
Bonetto, M.C., Sacco, N.J., Ohlsson, A.H., Corton, E., Sticker, D., Charwat, V., Ertl, P., 2014. Rapid and label-free differentiation of bacterial strains using low frequency electrochemical impedance spectroscopy. IEEE 1–4.
Brakstad, O.G., Aasbakk, K., Maeland, J.A., 1992. Detection of *Staphylococcus aureus* by polymerase chain reaction amplification of the nuc gene. J. Clin. Microbiol. 30, 1654–1660.
Bringans, R.D., Höchst, H., Shanks, H.R., 1981. Defect states in WO_3 studied with photoelectron spectroscopy. Phys. Rev. B 24, 3481–3489.
Chen, S.M., Li, Y., Hsu, Z.C., 2012. Multi-functionalized biosensor at WO_3–TiO_2 modified electrode for photoelectrocatalysis of norepinephrine and riboflavin. Sensor. Actuator. B Chem. 174, 427–435.
CLSI, 2015. Methods for Dilution Antimicrobial Susceptibility Tests for Bacteria that Grow aerobically. CLSI Document M07-A8. Clinical and Laboratory Standards Institute, Wayne.

Daniels, J.S., Pourmand, N., 2007. Label-free impedance biosensors: opportunities and challenges. Electroanalysis 19, 1239–1257.
Deb, S.K., 1973. Optical and photoelectric properties and colour centres in thin films of tungsten oxide. Philos. Mag. A 27, 801–822.
Ensom, M.H.H., Decarie, D., Lakhani, A., 2010. Stability of vancomycin 25 mg/mL in orasweet and water in unit-dose cups and plastic bottles at 4°C and 25°C. Can. J. Hosp. Pharm. 63 (5), 366–372.
Etayash, H., Jiang, K., Thundat, T., Kaur, K., 2014. Impedimetric detection of pathogenic Gram-positive bacteria using an antimicrobial peptide from class IIa bacteriocins. Anal. Chem. 86 (3), 1693–1700.
Freed, R.C., Evenson, M.L., Reiser, R.F., Bergdoll, M.S., 1982. Enzyme-linked immunosorbent assay for detection of staphylococcal enterotoxins in foods. Appl. Environ. Microbiol. 44, 1349–1355.
Gillet, M., Lemire, C., Gillet, E., Aguir, K., 2003. The role of surface oxygen vacancies upon WO_3 conductivity. Surf. Sci. 532–535, 519–525.
Goel, S., Mishra, P., 2018. Thymoquinone inhibits biofilm formation and has selective antibacterial activity due to ROS generation. Appl. Microbiol. Biotechnol. 102, 1955–1967.
Herceg, Z., Jambrak, A.R., Lelas, V., Thagard, S.M., 2013. The effect of high intensity ultrasound treatment on the amount of *Staphylococcus aureus* and *Escherichia coli* in Milk. Food Technol. Biotechnol. 51 (3), 352–359.
Hoyos-Nogués, M., Brosel-Oliu, S., Abramova, N., Muñoz, F.-X., Bratov, A., Mas-Moruno, C., Gil, F.-J., 2016. Impedimetric antimicrobial peptide-based sensor for the early detection of periodontopathogenic bacteria. Biosens. Bioelectron. 86, 377–385.
Hu, M., Zeng, J., Wang, W., Chen, H., Qin, Y., 2012. NO_2-sensing properties of porous WO_3 gas sensor based on anodized sputtered tungsten thin film. Sensor. Actuator. B Chem. 161, 447–452.
Hubbard, B.K., Walsh, C.T., 2003. Vancomycin assembly: nature's way. Angew. Chem. Int. Ed. 42, 730–765.
Jaiswal, S., Mishra, P., 2018. Antimicrobial and antibiofilm activity of curcumin-silver nanoparticles with improved stability and selective toxicity to bacteria over mammalian cells. Med. Microbiol. Immunol. 207, 39–53.
Jia, F., Duan, N., Wu, S., Ma, X., Xia, Y., Wang, Z., Wei, X., 2014. Impedimetric aptasensor for *Staphylococcus aureus* based on nanocomposite prepared from reduced graphene oxide and gold nanoparticles. Microchim. Acta. 181, 967–974.
Joyce, E., Phull, S.S., Lorimer, J.P., Mason, T.J., 2003. The development and evaluation of ultrasound for the treatment of bacterial suspensions. A study of frequency, power and sonication time on cultured *Bacillus* species. Ultrason. Sonochem. 10, 315–318.
Kalyani, N., Moudgil, A., Das, S., Mishra, P., 2017. Metalloprotein based scalable field effect transistor with enhanced switching behaviour. Sensor. Actuator. B Chem. 246, 363–369.
Kell, A.J., Stewart, G., Ryan, S., Peytavi, R., Boissinot, M., Huletsky, A., Bergeron, M.G., Simard, B., 2008. Vancomycin-modified nanoparticles for efficient targeting and preconcentration of Gram-positive and Gram-negative bacteria. ACS Nano 2, 1777–1788.
Koubová, V., Brynda, E., Karasová, L., Škvor, J., Homola, J., Dostálek, J., Tobiška, P., Rošický, J., 2001. Detection of foodborne pathogens using surface plasmon resonance biosensors. Sensor. Actuator. B Chem. 74, 100–105.
Kumar, S., Lodhi, D.K., Goel, P., Neeti, Mishra, P., Singh, J.P., 2015. A facile method for fabrication of buckled PDMS silver nanorod arrays as active 3D SERS cages for bacterial sensing. Chem. Commun. 51, 12411–12414.
Kwon, Y.T., Yong, K., Lee, W., Choi, G., Do, Y., 2000. Photocatalytic behavior of WO_3 loaded TiO_2 in an oxidation reaction. J. Catal. 191, 192–199.
Li, R., Goswami, U., King, M., Chen, J., Cesario, T.C., Rentzepis, P.M., 2018. In situ detection of live-to-dead bacteria ratio after inactivation by means of synchronous fluorescence and PCA. Proc. Natl. Acad. Sci. U. S. A 115, 668–673.
Li, W.J., Fu, Z.W., 2010. Nanostructured WO_3 thin film as a new anode material for lithium-ion batteries. Appl. Surf. Sci. 256, 2447–2452.
Li, Y., Afrasiabi, R., Fathi, F., Wang, N., Xiang, C., Love, R., She, Z., Kraatz, H.B., 2014. Impedance based detection of pathogenic *E. coli* O157:H7 using a ferrocene-antimicrobial peptide modified biosensor. Biosens. Bioelectron. 58, 193–199.
Li, Y., Wang, R., Ruan, C., Kanayeva, D., Lassiter, K., 2008. TiO_2 nanowire bundle microelectrode based impedance immunosensor for rapid and sensitive detection of *Listeria monocytogenes*. Nano Lett. 8, 9.
Lin, C.C., Yeh, Y.C., Yang, C.Y., Chen, C.L., Chen, G.F., Chen, C.C., Wu, Y.C., 2002. Selective binding of mannose-encapsulated gold nanoparticles to type 1 pili in *Escherichia coli*. J. Am. Chem. Soc. 124, 3508–3509.
Lin, Y.S., Tsai, P.J., Weng, M.F., Chen, Y.C., 2005. Affinity capture using vancomycin-bound magnetic nanoparticles for the MALDI-MS analysis of bacteria. Anal. Chem. 77, 1753–1760.
Liu, T.Y., Tsai, K.T., Wang, H.H., Chen, Y., Chen, Y.H., Chao, Y.C., Chang, H.H., Lin, C.H., Wang, J.K., Wang, Y.L., 2011. Functionalized arrays of Raman-enhancing nanoparticles for capture and culture-free analysis of bacteria in human blood. Nat. Commun. 2, 538.
Lu, X., Samuelson, D.R., Xu, Y., Zhang, H., Wang, S., Rasco, B.A., Xu, J., Konkel, M.E., 2013. Detecting and tracking nosocomial methicillin-resistant *Staphylococcus aureus* using a microfluidic SERS biosensor. Anal. Chem. 85, 2320–2327.
Miller, J.N., Miller, J.C., 2005. Statistics and Chemometrics for Analytical Chemistry. Pearson, England .
Moudgil, A., Dhyani, V., Das, S., 2018a. High speed efficient ultraviolet photodetector based on 500 nm width multiple WO_3 nanowires. Appl. Phys. Lett. 113, 101101.
Moudgil, A., Kalyani, N., Sinsinbar, G., Das, S., Mishra, P., 2018b. S-layer protein for resistive switching and flexible nonvolatile memory device. ACS Appl. Mater. Interfaces 10, 4866–4873.
Ohno, T., Tanigawa, F., Fujihara, K., Izumi, S., Matsumura, M., 1998. Photocatalytic oxidation of water on TiO_2-coated WO_3 particles by visible light using iron (III) ions as electron acceptor. J. Photochem. Photobiol. A Chem. 118, 41–44.
Owen, J.F., Teegarden, K.J., Shanks, H.R., 1978. Optical properties of the sodium-tungsten bronzes and tungsten trioxide. Phys. Rev. B 18, 3827–3837.
Pfeiffer, R.R., 1981. Structural Features of Vancomycin, Source: Reviews of Infectious Diseases, vol. 3.
Piyasena, P., Mohareb, E., McKellar, R., 2003. Inactivation of microbes using ultrasound: a review. Int. J. Food Microbiol. 87, 207–216.
Rao, J., Colton, I.J., Whitesides, G.M., 1997. Using capillary electrophoresis to study the electrostatic interactions involved in the association of D-Ala-D-Ala with vancomycin. J. Am. Chem. Soc. 119, 9336–9340.
Ranjbar, S., Shahrokhian, S., 2018. Design and fabrication of an electrochemical aptasensor using Au nanoparticles/carbon nanoparticles/cellulose nanofibers nanocomposite for rapid and sensitive detection of *Staphylococcus aureus*. Bioelectrochemistry 123, 70–76.
Reich, P., Stoltenburg, R., Strehlitz, B., Frense, D., Beckmann, D., Stoltenburg, R., Strehlitz, B., Frense, D., Beckmann, D., 2017. Development of an impedimetric aptasensor for the detection of *Staphylococcus aureus*. Int. J. Mol. Sci. 18, 2484.
Ruan, C., Yang, L., Li, Y., 2002. Immunobiosensor chips for detection of *Escherichia coli* O157:H7 using electrochemical impedance spectroscopy. Anal. Chem. 74, 4814–4820.
Settu, K., Chen, C.J., Liu, J.T., Chen, C.L., Tsai, J.Z., 2015. Impedimetric method for measuring ultra-low *E. coli* concentrations in human urine. Biosens. Bioelectron. 66, 244–250.
Siciliano, T., Tepore, A., Micocci, G., Serra, A., Manno, D., Filippo, E., 2008. WO_3 gas sensors prepared by thermal oxidization of tungsten. Sensor. Actuator. B Chem. 133, 321–326.
Solanki, P.R., Kaushik, A., Agrawal, V.V., Malhotra, B.D., 2011. Nanostructured metal oxide-based biosensors. NPG Asia Mater. 3, 17–24.
Shahrokhian, S., Ranjbar, S., 2018. Aptamer immobilization on amino-functionalized metal-organic frameworks: an ultrasensitive platform for the electrochemical diagnostic of *Escherichia coli* O157:H7. Analyst 143, 3191–3201.
Sundram, U.N., Griffin, J.H., Nicas, T.I., 1996. Novel vancomycin dimers with activity against vancomycin-resistant *Enterococci*. J. Am. Chem. Soc. 118, 13107–13108.
Soukka, T., Härmä, H., Paukkunen, J., Lövgren, T., 2001. Utilization of kinetically enhanced monovalent binding affinity by immunoassays based on multivalent nanoparticle-antibody bioconjugates. Anal. Chem. 73, 2254–2260.
Templier, V., Roux, A., Roupioz, Y., Livache, T., 2016. Ligands for label-free detection of whole bacteria on biosensors: a review. Trends Anal. Chem. 79, 71–79.
Topoglidis, E., Cass, A.E.G., Gilardi, G., Sadeghi, S., Beaumont, N., Durrant, J.R., 1998. Protein adsorption on nanocrystalline TiO_2 Films: an immobilization strategy for bioanalytical devices. Anal. Chem. 70, 5111–5113.
Wang, F., Zhou, H., Olademehin, O.P., Kim, S.J., Tao, P., 2018. Insights into key interactions between vancomycin and bacterial cell wall structures. ACS Omega 3, 37–45.
Wang, Y., Ping, J., Ye, Z., Wu, J., Ying, Y., 2013. Impedimetric immunosensor based on gold nanoparticles modified graphene paper for label-free detection of *Escherichia coli* O157:H7. Biosens. Bioelectron. 49, 492–498.
Wang, Z., Zhang, J., Chen, P., Zhou, X., Yang, Y., Wu, S., Niu, L., Han, Y., Wang, L., Chen, P., Boey, F., Zhang, Q., Liedberg, B., Zhang, H., 2011. Label-free, electrochemical detection of methicillin-resistant *Staphylococcus aureus* DNA with reduced graphene oxide-modified electrodes. Biosens. Bioelectron. 26, 3881–3886.
Ward, A.C., Hannah, A.J., Kendrick, S.L., Tucker, N.P., MacGregor, G., Connolly, P., 2018. Identification and characterisation of *Staphylococcus aureus* on low cost screen printed carbon electrodes using impedance spectroscopy. Biosens. Bioelectron. 110, 65–70.
Wu, R., Ma, Y., Pan, J., Lee, S.H., Liu, J., Zhu, H., Gu, R., Shea, K.J., Pan, G., 2018. Efficient capture, rapid killing and ultrasensitive detection of bacteria by a nano-decorated multi-functional electrode sensor. Biosens. Bioelectron. 101, 52–59.
Wu, X., Huang, Y.W., Park, B., Tripp, R.A., Zhao, Y., 2015. Differentiation and classification of bacteria using vancomycin functionalized silver nanorods array based surface-enhanced Raman spectroscopy and chemometric analysis. Talanta 139, 96–103.
Xu, M., Wang, R., Li, Y., 2016. Rapid detection of *Escherichia coli* O157:H7 and *Salmonella typhimurium* in foods using an electrochemical immunosensor based on screen-printed interdigitated microelectrode and immunomagnetic separation. Talanta 148, 200–208.
Yang, C.C., Lin, C.C., Yen, S.K., 2011. Electrochemical deposition of Vancomycin/Chitosan composite on Ti alloy. J. Electrochem. Soc. 158 (12), 152–158.
Yang, H., Zhou, H., Hao, H., Gong, Q., Nie, K., 2016. Detection of *Escherichia coli* with a label-free impedimetric biosensor based on lectin functionalized mixed self-assembled monolayer. Sensor. Actuator. B Chem. 229, 297–304.
Yang, L., Li, Y., Griffis, C.L., Johnson, M.G., 2004a. Interdigitated microelectrode (IME) impedance sensor for the detection of viable *Salmonella typhimurium*. Biosens. Bioelectron. 19 (10), 1139–1147.
Yang, L., Li, Y., Erf, G.F., 2004b. Interdigitated array microelectrode-based electrochemical impedance immunosensor for detection of *Escherichia coli* O157:H7. Anal. Chem. 76, 1107–1113.
Zeng, J., Hu, M., Wang, W., Chen, H., Qin, Y., 2012. NO_2-sensing properties of porous WO_3 gas sensor based on anodized sputtered tungsten thin film. Sensor. Actuator. B Chem. 161, 447–452.
Zhang, J., Tu, J., Du, G., Dong, Z., Wu, Y., Chang, L., Xie, D., Cai, G., Wang, X., 2013. Ultra-thin WO_3 nanorod embedded polyaniline composite thin film: synthesis and electrochromic characteristics. Sol. Energy Mater. Sol. Cells 114, 31–37.
Zhang, J., Tu, J., Zhang, D., Qiao, Y., Xia, X., Wang, X., Gu, C., 2011. Multicolor electrochromic polyaniline–WO_3 hybrid thin films: one-pot molecular assembling synthesis. J. Mater. Chem. 21, 17316.